

Optimal Beam Sweeping and Communication in Mobile Millimeter-Wave Networks

Nicolò Michelusi, Muddassar Hussain

Abstract

Millimeter-wave (mm-wave) communications incur a high beam alignment cost in mobile scenarios such as vehicular networks. Therefore, an efficient beam alignment mechanism is required to mitigate the resulting overhead. In this paper, a one-dimensional mobility model is proposed where a mobile user (MU), such as a vehicle, moves along a straight road with time-varying and random speed, and communicates with base stations (BSs) located on the roadside over the mm-wave band. To compensate for location uncertainty, the BS widens its transmission beam and, when a critical beamwidth is achieved, it performs beam-sweeping to refine the MU position estimate, followed by data communication over a narrow beam. The average rate and average transmission power are computed in closed form and the optimal beamwidth for communication, number of sweeping beams, and transmission power allocation are derived so as to maximize the average rate under an average power constraint. Structural properties of the optimal design are proved, and a bisection algorithm to determine the optimal sweeping – communication parameters is designed. It is shown numerically that an adaptation of the IEEE 802.11ad standard to the proposed model exhibits up to 90% degradation in spectral efficiency compared to the proposed scheme.

I. INTRODUCTION

Millimeter-wave (mm-wave) technology has emerged as a promising solution to enable multi-Gbps communication, thanks to the abundant bandwidth available [1]. Mm-wave will be key to supporting autonomous transportation systems by allowing vehicles to extend their sensing range and make more informed decisions by exchanging rich sensory information [2]. It will also enable a wide range of infotainment services such as digital maps, cloud computing, ultra-high definition video streaming, etc. However, signal propagation at these frequencies poses several

N. Michelusi and M. Hussain are with the School of Electrical and Computer Engineering at Purdue University. Email: {michelus, hussai13}@purdue.edu.

This research has been funded by the National Science Foundation under grant CNS-1642982.

challenges to the design of future communication systems supporting high throughput and high mobility, such as high isotropic path loss and sensitivity to blockages [3]. Mm-wave systems are expected to leverage narrow-beam communications to counteract the propagation loss [4] by using large antenna arrays at both base stations (BSs) and mobile users (MUs).

However, sharp beams are susceptible to beam mis-alignment due to mobility or blockage, necessitating frequent re-alignment. This task can be challenging, especially in mobile scenarios. The beam alignment protocol may consume time, frequency, and energy resources, thus potentially offsetting the benefits of mm-wave directionality. Therefore, it is imperative to design schemes to mitigate its overhead.

In this paper, we investigate the trade-off between beam alignment and data communication in mobile mm-wave networks. We propose a beam-sweeping – data communication protocol that accounts for the uncertainty on the location and speed of the MU and for the temporal overhead of beam-sweeping. Specifically, the BS associated with the MU widens its transmission beam to compensate for the increasing uncertainty on the MU location and, when a critical beamwidth is achieved, it performs beam-sweeping to refine the MU’s position estimate and achieve a narrow communication beam. We compute the performance in closed-form, and investigate the design of the optimal beamwidth for communication, number of sweeping beams, and transmission power so as to maximize the average rate under average power constraint. We find structural properties and propose a bisection method to determine the optimal design. We show numerically that an adaptation of IEEE 802.11ad to our model exhibits a performance degradation up to 90% compared to our design.

Beam alignment in mm-wave has been a subject of intensive research due to its importance in mm-wave communication systems. The research in this area can be categorized into beam-sweeping [5]–[8]; AoA/AoD estimation [9], [10]; and data-assisted schemes [2], [11]–[13]. Beam-sweeping based schemes require scanning of regions of uncertainty of AoA/AoD. The simplest and yet most popular form of beam-sweeping is the so-called *exhaustive* search [5], which sequentially scans through all possible beam pairs from the BS and MU codebooks and selects the one with maximum signal power. This approach has been adopted in existing mm-wave standards including IEEE 802.15.3c [14] and IEEE 802.11ad [15]. The other popular scheme is a hierarchical form of scanning called *iterative* search [6], where beam-sweeping is first performed using wider beams followed by refinement with narrow beams. In our previous work [8], we derived an energy-efficient scheme termed *fractional search*, which minimizes the

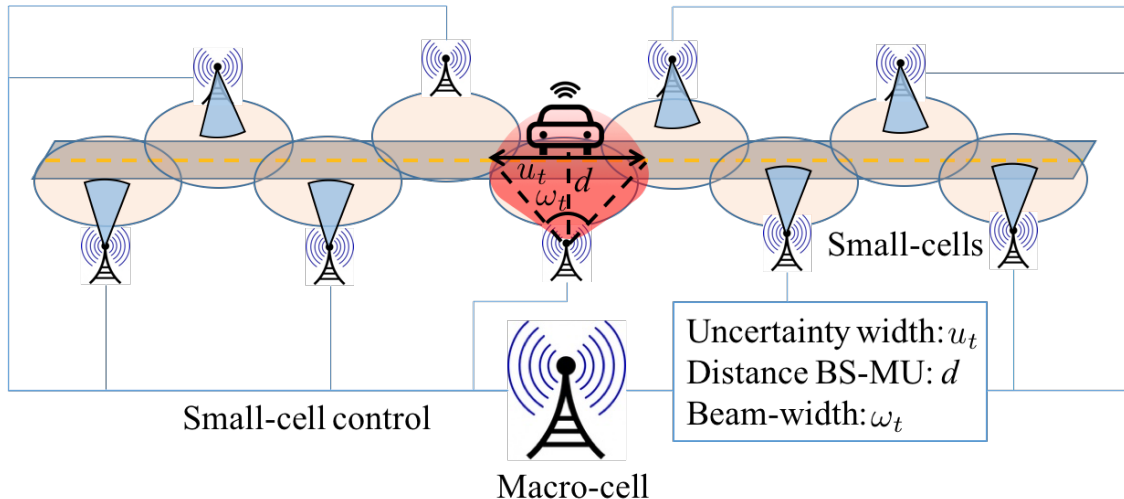


Fig. 1: System model.

energy consumption subject to a rate constraint: in each slot, the BS adaptively scans a fraction of the uncertainty region of the AoD, function of the slot index, rate requirement, probabilities of false-alarm and mis-detection, bandwidth, path loss, and noise power spectral density.

AoA/AoD estimation aims to reduce the number of measurements required by beam-sweeping by leveraging the sparsity of mm-wave channels, *e.g.*, via compressive sensing as in [9]. The paper [10] derived an approximate maximum likelihood estimator for the channel by directly exploiting the structure of the mm-wave channel. Data-aided schemes utilize information from radar [11], lower frequencies [12], or positional information [2], [13] to reduce the cost of beam-sweeping. Based on this idea, the authors of [2] proposed a beamwidth optimization algorithm that maximizes the data rate for non-overlapping beams. In contrast to [2], we propose an analytical framework for the joint optimization of beamwidth, communication power and beam-sweeping to maximize the communication performance. *To the best of our knowledge, we are the first to propose an analytical framework for the optimization of the beam-sweeping and communication parameters in mobile mm-wave networks.*

The paper is organized as follows: in Sec. II, we present the system model and optimization problem; in Sec. III, we present the analysis, followed by numerical results in Sec. IV; finally, in Sec. V, we conclude with some remarks.

II. SYSTEM MODEL

We consider a *dense* cell deployment, as depicted in Fig. 1. The MU is associated with its closest BS, at distance d . We assume that the BS points its beam perpendicularly to the motion of the MU (a good approximation in dense cell deployments). A macro-cell unit controls functions such as handover among cells. The time-scale of this task is larger than the beam-sweeping – data communication cycle, and thus we neglect it. We neglect the additional overhead due to channel estimation, Doppler correction, and the impact of beamwidth on Doppler spread (see [16]).

A. User mobility model

The MU moves along a line (*e.g.*, a vehicle along a road). Let $(p_t, v_t) \in \mathbb{R}^2$ be its position and speed at time t . We assume that $v_t \in [v_{\min}, v_{\max}]$, where $v_{\min} < v_{\max}$ (possibly, negative), and we let $v_{\text{drift}} = (v_{\min} + v_{\max})/2$ be the drift velocity and $\phi \triangleq v_{\max} - v_{\min}$ be the speed uncertainty. v_t is time-varying and random, with *arbitrary* distribution in $[v_{\min}, v_{\max}]$. The speed parameters v_{drift}, ϕ are assumed to be known, and can be estimated from GPS information collected at the macro-cell (*e.g.*, via lower frequency dedicated short range communication channels [17]). Herein, we assume that $v_{\text{drift}} = 0$, since a known non-zero drift can be incorporated by appropriate beam steering. Thus, it follows that $v_t \in [-\phi/2, \phi/2]$ and, given p_0 at a reference time 0,

$$p_t = p_0 + \int_0^t v_\tau d\tau \in \left[p_0 - \frac{\phi t}{2}, p_0 + \frac{\phi t}{2} \right]. \quad (1)$$

In this paper, the uncertainty on the location of the MU at time t is denoted by the *uncertainty interval* $\mathcal{U}_t \equiv [\hat{p}_t - u_t/2, \hat{p}_t + u_t/2]$, where \hat{p}_t is the median estimated position and u_t is the *uncertainty width*, so that $p_t \in \mathcal{U}_t$. From the mobility model (1), if no beam-sweeping is done in the time interval $[t, \tau]$, the uncertainty width augments at rate ϕ , *i.e.*,

$$u_\tau = u_t + \phi(\tau - t), \quad \tau \geq t, \quad (2)$$

and is reduced via beam-sweeping, as discussed in Sec. II-B.

The communication between BS and MU follows a beam-sweeping – data communication cycle of duration T . We now describe the entire cycle, starting from the reference time $t=0$.

B. Beam Sweeping

When, at the reference time $t = 0$, the uncertainty width reaches a critical value $u_0 = u_{\text{th}}$, the BS currently associated with the MU sweeps the entire uncertainty interval \mathcal{U}_0 using $\eta \geq 2, \eta \in \mathbb{N}$ beams, transmitted sequentially over η microslots, each of duration δ_S . During this interval, the uncertainty width increases over time due to MU mobility. In order to compensate for it, the BS scans wider regions over successive microslots, as detailed below. Thus, we let ω_i be the beamwidth of the i th beam, where $i = 1, 2, \dots, \eta$.

At the end of the beam-sweeping interval of duration $\eta\delta_S$, the MU processes the signals, and feeds back to the BS the ID of the strongest signal (e.g., via a lower frequency control channel). The BS uses such strongest beam to communicate with the MU in the data communication phase, as detailed in Sec. II-C. We neglect the time to send this feedback signal.

$\{\omega_i, i = 1, 2, \dots, \eta\}$ are designed with the following requirements: **R1** – By the end of the beam-sweeping phase, the entire uncertainty interval \mathcal{U}_0 must be scanned, plus the additional uncertainty resulting from the MU mobility during the beam-sweeping phase; **R2** – the beamwidth at the beginning of the data communication phase, $u_{\eta\delta_S}$, must be independent of the strongest beam selected.

To guarantee **R2**, note that, if the i th beam, $i = 1, 2, \dots, \eta$ is the strongest one detected (with beamwidth ω_i), the uncertainty width at the end of the beam-sweeping phase becomes¹

$$u_{\eta\delta_S} = d\omega_i + (\eta + 1 - i)\delta_S\phi, \quad (3)$$

due to the MU mobility in the subsequent $(\eta + 1 - i)$ microslots until the end of beam-sweeping. Hence, **R2** requires

$$\omega_i = \omega_1 + (i - 1)\frac{\delta_S\phi}{d}, \quad \forall i = 1, 2, \dots, \eta, \quad (4)$$

so that, at the end of beam-sweeping, the uncertainty width becomes

$$u_{\eta\delta_S} = d\omega_1 + \eta\delta_S\phi, \quad \forall i. \quad (5)$$

We now discuss how to design ω_1 (and ω_i via (4)) so as to guarantee **R1**. At the reference time 0, the uncertainty interval is $[0, u_{\text{th}}]$. In the first microslot, the BS scans the interval $[0, d\omega_1]$

¹Herein, we assume that $\omega_i \ll 2\pi$, so that the length of the interval scanned in the i th microslot is $2d \tan(\omega_i/2) \simeq d\omega_i$, see Fig. 1 (the beam is approximated as being pointed perpendicularly to the motion of the MU).

using a beam with beamwidth ω_1 . If the MU is within this interval, at the end of the beam-sweeping phase it will detect the ID of the strongest beam as #1, and the uncertainty width will thus be given by (5). Otherwise (if the MU is outside of this interval), after the first microslot the MU may be in the interval $[d\omega_1 - \delta_S\phi/2, u_{\text{th}} + \delta_S\phi/2]$, which accounts for the additional uncertainty due to the MU mobility in the time interval $[0, \delta_S]$. Thus, in the second microslot, the BS scans the interval $[d\omega_1 - \delta_S\phi/2, d\omega_1 + d\omega_2 - \delta_S\phi/2]$ using a beam with beamwidth ω_2 . If the MU is within this interval, at the end of the beam sweeping phase it will detect the ID of the strongest beam as #2, and the uncertainty width will thus be given by (5). Otherwise (if the MU is outside of this interval), after the second microslot the MU may be in the interval $[d\omega_1 + d\omega_2 - \delta_S\phi, u_{\text{th}} + \delta_S\phi]$, which accounts for the additional uncertainty due to the MU mobility in the time interval $[\delta_S, 2\delta_S]$. Thus, in the third microslot, the BS scans the interval $[d\omega_1 + d\omega_2 - \delta_S\phi, d\omega_1 + d\omega_2 + d\omega_3 - \delta_S\phi]$ with a beam with beamwidth equal to ω_3 , and so on.

By induction, at the beginning of the i th microslot, where $i = 1, 2, \dots, \eta$, $i-1$ beams have been scanned. If the MU was located within one of the previous $i-1$ beams (say the j th, $j \leq i-1$), it will detect the ID of the strongest beam as # j at the end of the beam-sweeping phase, and the uncertainty width will thus be given by (5). Otherwise (if the MU is located within one of the next beams $i, i+1, \dots, \eta$), the MU may be in the interval $[d \sum_{k=1}^{i-1} \omega_k - (i-1)\delta_S\phi/2, u_{\text{th}} + (i-1)\delta_S\phi/2]$ at the beginning of the i th microslot, which accounts for the additional uncertainty due to the MU mobility in the time interval $[0, (i-1)\delta_S]$. Thus, in the i th microslot, the BS scans the interval $[d \sum_{k=1}^{i-1} \omega_k - (i-1)\delta_S\phi/2, d \sum_{k=1}^i \omega_k - (i-1)\delta_S\phi/2]$ using a beam with beamwidth ω_i . If the MU is within this interval, it will detect the ID of the strongest beam as # i at the end of the beam-sweeping period, and the uncertainty width will thus be given by (5). Otherwise (if the MU is outside of this interval), at the end of the i th microslot the MU may be in the interval $[d \sum_{k=1}^i \omega_k - i\delta_S\phi/2, u_{\text{th}} + i\delta_S\phi/2]$, which accounts for the additional uncertainty due to the MU mobility in the time interval $[(i-1)\delta_S, i\delta_S]$.

Using a similar argument, in the last microslot (the η th one), if the MU was not located within one of the previous $\eta-1$ beams, then the MU will be located in the interval $[d \sum_{k=1}^{\eta-1} \omega_k - (\eta-1)\delta_S\phi/2, u_{\text{th}} + (\eta-1)\delta_S\phi/2]$ of width $u_{\text{th}} + (\eta-1)\delta_S\phi - d \sum_{k=1}^{\eta-1} \omega_k$. This must be scanned exhaustively with a beam of width ω_η , hence

$$d\omega_\eta = u_{\text{th}} + (\eta-1)\delta_S\phi - d \sum_{k=1}^{\eta-1} \omega_k. \quad (6)$$

By combining (6) with (4) we obtain, $\forall i = 1, 2, \dots, \eta$,

$$\omega_i = \frac{u_{\text{th}}}{d\eta} - \frac{(\eta-1)(\eta-2)}{2\eta} \frac{\delta_S \phi}{d} + (i-1) \frac{\delta_S \phi}{d}. \quad (7)$$

At the end of beam-sweeping, data communication begins and the new uncertainty width is given by (5), yielding

$$u_{\text{comm}}(u_{\text{th}}, \eta) \triangleq u_{\eta\delta_S} = \frac{u_{\text{th}}}{\eta} + \eta\delta_S\phi - \delta_S\phi \frac{(\eta-1)(\eta-2)}{2\eta}. \quad (8)$$

which evolves over the data communication interval according to (2).

Note that a feasible beam is such that $\omega_k \geq 0, \forall k = 1, 2, \dots, \eta$. Additionally, beam-sweeping must reduce the uncertainty width, *i.e.*, $u_{\text{comm}}(u_{\text{th}}, \eta) \leq u_{\text{th}}$. These two conditions together yield

$$u_{\text{th}} \geq \delta_S\phi \max \left\{ \frac{\eta^2/2 + 3/2\eta - 1}{\eta - 1}, \frac{1}{2}(\eta - 1)(\eta - 2) \right\}. \quad (9)$$

Herein, we assume that the correct sector is detected with no error by the MU (this requires proper beam design to achieve small false-alarm and misdetection probabilities, see [18]).

C. Data communication

Immediately after beam-sweeping, at time $t = \eta\delta_S$, the data communication phase begins, and the uncertainty width is $u_{\eta\delta_S} = u_{\text{comm}}(u_{\text{th}}, \eta)$. The uncertainty width u_t increases over time due to the mobility of the MU, according to (2). The data communication period, and the beam-sweeping – data communication cycle, terminate at time T such that $u_T = u_{\text{th}}$, at which time a new cycle begins. From (2) we obtain

$$T = \frac{(\eta-1)u_{\text{th}}}{\phi\eta} + \frac{\delta_S}{2} \frac{(\eta-1)(\eta-2)}{\eta}. \quad (10)$$

In the time interval $[\eta\delta_S, T]$, the transmission beam of the BS associated with the MU is chosen so as to support reliable communication over the entire uncertainty interval. Its beamwidth is thus chosen as $\omega_t \simeq u_t/d$ [rad].²

Remark 1. Note that in our model the beamwidth is varied continuously within a continuous set $\omega \in [u_{\text{comm}}(u_{\text{th}}, \eta)/d, u_{\text{th}}/d]$ for analytical tractability. This approach is a continuous ap-

²Note that we assume that $u_t/d \ll 2\pi$, so that we can approximate the beamwidth as $\omega_t = 2 \arctan(u_t/d/2) \simeq u_t/d$, see Fig. 1.

proximation of a practical deployment where the system may operate at discrete times using a discrete codebook to generate transmission beams with different beamwidths [19].

Let P_t be the transmission power per Hz at time t to communicate reliably. Assuming isotropic reception at the MU [7], [8], the instantaneous transmission rate is given by

$$R_t = W_{\text{tot}} \log_2 \left(1 + \gamma \frac{P_t}{\omega_t} \right), \quad (11)$$

where W_{tot} is the bandwidth, $\gamma \triangleq \frac{\lambda^2 \xi}{8\pi d^2 N_0 W_{\text{tot}}}$ is the SNR scaling factor, λ is the wavelength, N_0 is the noise power spectral density, and ξ is the antenna efficiency. Note that P_t is spread evenly across the angular directions covered by the transmission beams, so that P_t/ω_t is the power per radian delivered to the receiver.

D. Performance metrics and optimization problem

The optimal choice of the beam-sweeping and communication parameters reflects a trade-off between locating the MU with high accuracy so as to achieve narrow-beam communication, and mitigating the overhead in terms of sweeping time. This is the goal of our design.

Let $\eta \geq 2$, $\eta \in \mathbb{N}$, u_{th} satisfying (9), and $P : [\eta\delta_S, T] \mapsto \mathbb{R}_+$ be the transmit power function in the data communication phase. We define the time-average communication rate and transmission power, defined over one beam-sweeping – data communication cycle $[0, T]$, as

$$\bar{R}(\eta, u_{\text{th}}, P) = \frac{W_{\text{tot}}}{T} \int_{\eta\delta_S}^T \log_2 \left(1 + \frac{d\gamma P_t}{u_{\text{comm}}(u_{\text{th}}, \eta) + \phi t} \right) dt, \quad (12)$$

$$\bar{P}(\eta, u_{\text{th}}, P) = \frac{W_{\text{tot}}}{T} \int_{\eta\delta_S}^T P_t dt. \quad (13)$$

The goal is to determine the optimal design of the joint data communication and beam-sweeping parameters (η, u_{th}, P) so as to maximize the average rate under average power constraint $P_{\text{max}} > 0$, *i.e.*,

$$\mathbf{P1} : \quad (\eta, u_{\text{th}}, P)^* = \arg \max_{(\eta, u_{\text{th}}, P)} \bar{R}(\eta, u_{\text{th}}, P), \quad (14)$$

$$\text{s.t.} \quad \bar{P}(\eta, u_{\text{th}}, P) \leq P_{\text{max}}. \quad (15)$$

The analysis is carried out in the next section.

III. ANALYSIS

Due to the concavity of the \log_2 function, Jensen's inequality yields the following result.

Lemma 1. The optimal power allocation function $P : [\eta\delta_S, T] \mapsto \mathbb{R}_+$ is given by the water-filling scheme

$$P_t = \left(\rho - \frac{u_t}{d\gamma} \right)^+, \quad \forall t \in [\eta\delta_S, T], \quad (16)$$

where $\rho \geq \frac{u_{\text{comm}}(u_{\text{th}}, \eta)}{d\gamma}$ is a parameter to optimize. \square

Under the water-filling power allocation, the design space is simplified to $(\eta, u_{\text{th}}, \rho)$, where $\eta \geq 2, \eta \in \mathbb{N}$, u_{th} satisfies (9), and $\rho \geq \frac{u_{\text{comm}}(u_{\text{th}}, \eta)}{d\gamma}$. The average rate and average transmission power can be computed in closed form and are given by³

$$\begin{aligned} \bar{R}(\eta, u_{\text{th}}, \rho) = & \frac{W_{\text{tot}}}{\ln(2)\phi T} \left[\left(u_{\text{th}} - u_{\text{comm}}(u_{\text{th}}, \eta) \right) \left(1 + \ln(d\gamma\rho) \right) \right. \\ & - u_{\text{th}} \ln(u_{\text{th}}) + u_{\text{comm}}(u_{\text{th}}, \eta) \ln(u_{\text{comm}}(u_{\text{th}}, \eta)) \\ & \left. + \chi(d\gamma\rho \leq u_{\text{th}}) \left(u_{\text{th}} \ln\left(\frac{u_{\text{th}}}{d\gamma\rho}\right) + d\gamma\rho - u_{\text{th}} \right) \right], \end{aligned} \quad (17)$$

$$\begin{aligned} \bar{P}(\eta, u_{\text{th}}, \rho) = & \chi(d\gamma\rho \leq u_{\text{th}}) \frac{(u_{\text{th}} - d\gamma\rho)^2}{2d\phi\gamma T} \\ & + \frac{u_{\text{th}} - u_{\text{comm}}(u_{\text{th}}, \eta)}{2d\phi\gamma T} \left(2d\gamma\rho - u_{\text{th}} - u_{\text{comm}}(u_{\text{th}}, \eta) \right), \end{aligned} \quad (18)$$

where $\chi(\cdot)$ denotes the indicator function.

It is useful to define the following change of variables:

$$v \triangleq \frac{u_{\text{th}}}{\delta_S\phi}, \quad (19)$$

$$\zeta \triangleq \frac{d\gamma\rho}{\delta_S\phi v} - 1 \geq \frac{u_{\text{comm}}(u_{\text{th}}, \eta)}{\delta_S\phi v} - 1. \quad (20)$$

³We replace the dependence on the power allocation function P with the parameter ρ .

The performance metrics (17)-(18) can thus be expressed as

$$\hat{u}_{\text{comm}}(v, \eta) \triangleq \frac{u_{\text{comm}}(u_{\text{th}}, \eta)}{\delta_S \phi} = \frac{v}{\eta} + \frac{1}{2}\eta + \frac{3}{2} - \frac{1}{\eta}, \quad (21)$$

$$\hat{R}(\eta, v, \zeta) \triangleq \frac{\ln(2)}{W_{\text{tot}}} \bar{R}(\eta, u_{\text{th}}, \rho) = \frac{\eta}{\eta-1} \frac{1}{v + \frac{\eta}{2} - 1} \times \left[\left(v - \hat{u}_{\text{comm}}(v, \eta) \right) \left(1 + \ln(1 + \zeta) \right) \right. \quad (22)$$

$$\left. - \hat{u}_{\text{comm}}(v, \eta) \ln \left(\frac{v}{\hat{u}_{\text{comm}}(v, \eta)} \right) + \chi(\zeta < 0) v (\zeta - \ln(1 + \zeta)) \right],$$

$$\hat{P}(\eta, v, \zeta) \triangleq \frac{d\gamma}{\delta_S \phi} \bar{P}(\eta, u_{\text{th}}, \rho) = \frac{\eta v^2 \zeta^2 \chi(\zeta < 0)}{2(\eta-1)(v + \frac{\eta}{2} - 1)} + \frac{\eta(v - \hat{u}_{\text{comm}}(v, \eta))}{2(\eta-1)(v + \frac{\eta}{2} - 1)} \left(2v(1 + \zeta) - v - \hat{u}_{\text{comm}}(v, \eta) \right), \quad (23)$$

where (9) and $\rho \geq \frac{u_{\text{comm}}(u_{\text{th}}, \eta)}{d\gamma}$ yield the feasible set

$$\mathcal{F}_\eta \equiv \left\{ (v, \zeta) : v \geq v_{\min}(\eta), \zeta \geq \frac{\hat{u}_{\text{comm}}(v, \eta)}{v} - 1 \right\},$$

and we have defined

$$v_{\min}(\eta) \triangleq \max \left\{ \frac{\eta^2 + 3\eta - 2}{2(\eta-1)}, \frac{1}{2}(\eta-1)(\eta-2) \right\}. \quad (24)$$

Note that we have normalized the average rate and transmission power, so that they no longer depend on the system parameters $W_{\text{tot}}, \phi, d, \gamma, \delta_S$. This is beneficial since it unifies the structure of the optimal design in a wide range of scenarios.

The optimization problem thus becomes

$$\mathbf{P2} : (\eta, v, \zeta)^* = \arg \max_{\eta \geq 2, \eta \in \mathbb{N}, (v, \zeta) \in \mathcal{F}_\eta} \hat{R}(\eta, v, \zeta) \quad (25)$$

$$\text{s.t. } \hat{P}(\eta, v, \zeta) \leq \hat{P}_{\max}, \quad (26)$$

where $\hat{P}_{\max} = \frac{d\gamma}{\delta_S \phi} P_{\max}$. This optimization problem is non-convex. We have the following structural result.

Theorem 1. $\zeta < 0$ is suboptimal.

Proof. See Appendix A. □

The intuition behind Theorem 1 is that, if $\zeta < 0$, then the water-filling power allocation is such that $P_t = 0$ during a portion of the data communication phase. This is suboptimal: it is more energy-efficient to reduce the beam-sweeping threshold u_{th} and increase ζ so as to reduce the "idle" time interval in the communication phase.

Thus, in the following we focus on the case $\zeta \geq 0$. Note that $\hat{P}(\eta, v, \zeta)$ needs to satisfy the power constraint. Since it is an increasing function of ζ , we must have $\hat{P}(\eta, v, 0) \leq \hat{P}_{\max}$ to obtain a feasible solution, yielding

$$v \leq \frac{\eta^2 + 3\eta - 2}{2(\eta - 1)} + \frac{\eta \hat{P}_{\max}}{\eta - 1} \left(1 + \sqrt{1 + \frac{2\eta}{\hat{P}_{\max}}} \right) \triangleq v_{\max}(\eta). \quad (27)$$

Note that v must also satisfy the constraint $v \geq v_{\min}(\eta)$, hence we must have $v_{\max}(\eta) \geq v_{\min}(\eta)$. If $\eta \leq 4$, then $\frac{1}{2} \frac{\eta^2 + 3\eta - 2}{\eta - 1} > \frac{1}{2}(\eta - 1)(\eta - 2)$ and any v satisfying (27) also satisfies $v \geq v_{\min}(\eta)$. On the other hand, if $\eta \geq 5$ then $\frac{1}{2} \frac{\eta^2 + 3\eta - 2}{\eta - 1} < \frac{1}{2}(\eta - 1)(\eta - 2)$ and $v_{\max}(\eta) \geq v_{\min}(\eta)$ is equivalent to

$$\hat{P}_{\max} \geq \frac{1}{2} \frac{[\eta^2 - 5\eta + 2]^2}{\eta^2 - 4\eta + 2}, \text{ for } \eta \geq 5. \quad (28)$$

Since the right hand side is an increasing function of $\eta \geq 5$, we conclude that there exists $4 \leq \eta_{\max} < \infty$ such that the problem is feasible for all $2 \leq \eta \leq \eta_{\max}$ (indeed, the problem is always feasible for $\eta \in \{2, 3, 4\}$ since $v_{\max}(\eta) \geq v_{\min}(\eta)$ in this case). We thus define the new feasibility set as

$$\mathcal{F} \equiv \{(v, \eta) : 2 \leq \eta \leq \eta_{\max}, \eta \in \mathbb{N}, v_{\min}(\eta) \leq v \leq v_{\max}(\eta)\}.$$

Let $(v, \eta) \in \mathcal{F}$. Under such pair, $\hat{P}(\eta, v, \zeta)$ and $\hat{R}(\eta, v, \zeta)$ are increasing functions of $\zeta \geq 0$, hence the optimal ζ is such that the power constraint is attained with equality. We thus obtain ζ as a function of (v, η) as

$$\zeta(v, \eta) \triangleq \frac{(\eta - 1)(v + \eta/2 - 1)}{\eta v [v - \hat{u}_{\text{comm}}(v, \eta)]} (\hat{P}_{\max} - \hat{P}(0, \eta, v)). \quad (29)$$

Since the power constraint is satisfied with equality for $(v, \eta) \in \mathcal{F}$ and $\zeta = \zeta(v, \eta)$, the optimization problem becomes unconstrained, yielding

$$\mathbf{P3} : (\eta, v)^* = \arg \max_{(v, \eta) \in \mathcal{F}} \hat{R}(\eta, v, \zeta(v, \eta)), \quad (30)$$

and $\zeta^* = \zeta(v^*, \eta^*)$, where

$$\hat{R}(\eta, v, \zeta(v, \eta)) = \frac{\eta}{\eta - 1} \frac{1}{v + \frac{\eta}{2} - 1} \quad (31)$$

$$\begin{aligned} & \times \left[\left(v - \hat{u}_{\text{comm}}(v, \eta) \right) \left(1 + \ln(1 + \zeta(v, \eta)) \right) \right. \\ & \left. - \hat{u}_{\text{comm}}(v, \eta) \ln \left(\frac{v}{\hat{u}_{\text{comm}}(v, \eta)} \right) \right]. \end{aligned} \quad (32)$$

We solve the optimization problem as follows: for each $2 \leq \eta \leq \eta_{\max}$, we solve

$$v^*(\eta) = \arg \max_{v_{\min}(\eta) \leq v \leq v_{\max}(\eta)} \hat{R}(\eta, v, \zeta(v, \eta)). \quad (33)$$

Then, the optimal η^* and v^* are found by optimizing η via exhaustive search over the finite discrete set $\{2, 3, \dots, \eta_{\max}\}$,

$$\eta^* = \arg \max_{\eta \in \{2, 3, \dots, \eta_{\max}\}} \hat{R}(\rho(v^*(\eta), \eta), \eta, v^*(\eta)), \quad (34)$$

and $v^* = v^*(\eta^*)$.

A. Solution of (33) given $\eta \in \{2, 3, \dots, \eta_{\max}\}$

In this section, we investigate how to compute $v^*(\eta)$ given $\eta \in \{2, 3, \dots, \eta_{\max}\}$. We have the following theorem.

Theorem 2. Given $\eta \in \{2, 3, \dots, \eta_{\max}\}$, the optimal $v^*(\eta)$ is given by

$$v^*(\eta) = \max \left\{ \frac{1}{2}(\eta - 1)(\eta - 2), \hat{v} \right\}, \quad (35)$$

where \hat{v} is the unique solution in $(\frac{1}{2} \frac{\eta^2 + 3\eta - 2}{\eta - 1}, v_{\max}(\eta))$ of $f_\eta(v) = 0$, where

$$\begin{aligned} f_\eta(v) & \triangleq - \frac{v - \hat{u}_{\text{comm}}(v, \eta)}{v(1 + \rho(v, \eta))} \frac{(\eta - 1)(v + \eta/2 - 1) + 2\eta}{2\eta} \\ & - \frac{(\eta - 1)(v + \eta/2 - 1)}{\eta(1 + \rho(v, \eta))} \rho(v, \eta) \\ & + \ln(1 + \rho(v, \eta))\eta + \ln(v/\hat{u}_{\text{comm}}(v, \eta))(\eta/2 + 1). \end{aligned} \quad (36)$$

Proof. See Appendix B. □

The function $f_\eta(v)$ is proportional to the derivative of $\hat{R}(\eta, v, \zeta(v, \eta))$ with respect to v , up to a positive multiplicative factor. Note that \hat{v} can be determined using the bisection method. In fact, $f_\eta(v)$ is a decreasing function of v (see proof of the theorem in [20]), with

$$\lim_{v \rightarrow \frac{1}{2} \frac{\eta^2 + 3\eta - 2}{\eta - 1}} f_\eta(v) = \infty \text{ and } f_\eta(v_{\max}(\eta)) < 0. \quad (37)$$

IV. NUMERICAL RESULTS

In this section, we present numerical results to demonstrate the performance of the proposed beam-sweeping – data communication protocol. We compare our proposed scheme with an adaptation of IEEE 802.11ad to our model, in which partially overlapping beams of 7° beamwidth are employed such that adjacent beams share half of the beam area. Moreover, to evaluate this scheme we assume a worst-case scenario where the vehicle moves with either speed of v_{\max} or $v_{\min} = -v_{\max}$. Therefore, with IEEE 802.11ad, beam alignment is required after each r/v_{\max} [s] (the time required for the MU to move to the edge of the beam), where $r = d \tan(\frac{7^\circ}{2})$. Once the edge of the beam is reached (thus, the MU is located in either position $p \in \{-r, r\}$), the BS scans the two beams covering the intervals $[-2r, 0]$ and $[0, 2r]$, each with 7° beamwidth, so that the time overhead of beam sweeping is $2\delta_S$. Immediately after, the strongest beam is detected and data communication proceeds. Then, the fraction of time spent in data communication is given as

$$f_{\text{comm}} = \frac{r/v_{\max}}{r/v_{\max} + 2\delta_S}, \quad (38)$$

the average throughput of IEEE 802.11ad is given as

$$\bar{R}_{11\text{ad}} = W_{\text{tot}} \log_2 \left(1 + \gamma \frac{P_t}{7\pi/180} \right) \times f_{\text{comm}}, \quad (39)$$

TABLE I: Simulation parameters

Parameter	Symbol	Value
Carrier frequency	f_c	60 GHz
Bandwidth	W_{tot}	1.76 GHz
Noise PSD	N_0	-174 dBm/Hz
Microslot duration	δ_S	10 μ s
Distance BU-MU	d	10 m
Antenna efficiency	ξ	1

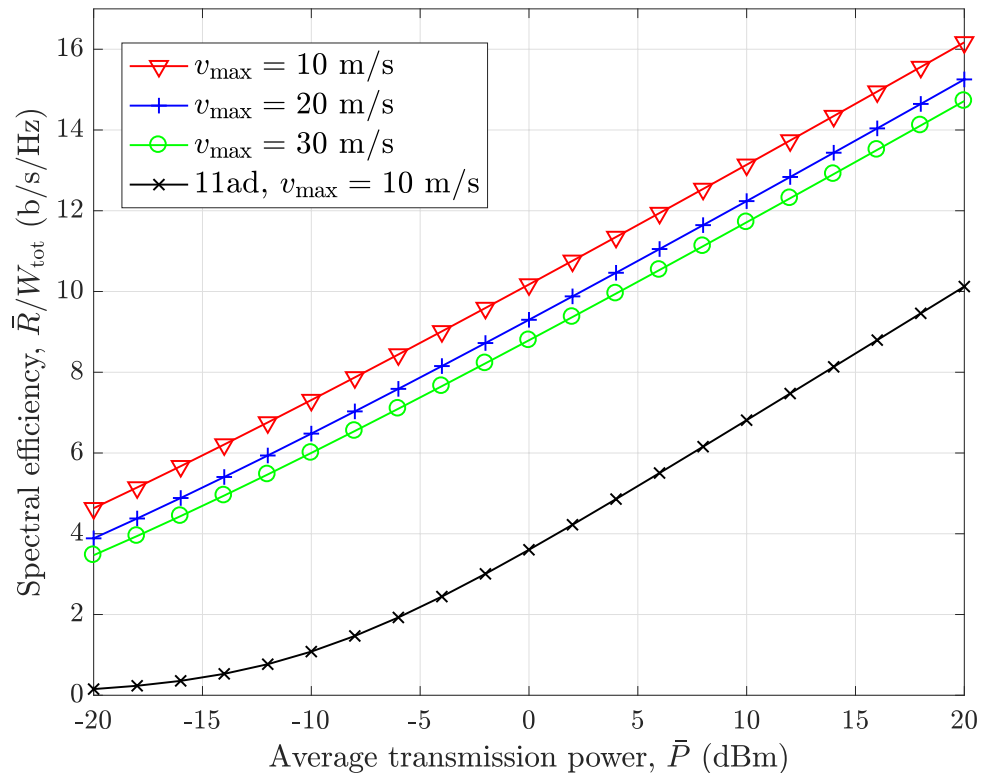


Fig. 2: Average spectral efficiency versus average power.

and the average power as $\bar{P}_{11\text{ad}} = P_t \times f_{\text{comm}}$. The common parameters of the simulation are given in Table I.

In Fig. 2, we plot the average spectral efficiency \bar{R}/W_{tot} versus the average power consumption \bar{P} . A monotonic trend between the spectral efficiency and the average power is observed. Moreover, the performance of the system deteriorates as we increase the speed, due to the increasing overhead of beam alignment. Additionally, we observe that IEEE 802.11ad performs poorly since it uses fixed 7° beams which are not optimized to the specific mobile scenario, with degradation up to 90% compared to our proposed scheme.

In Fig. 3, we plot the effect of speed on the spectral efficiency for two different values of the average power \bar{P} . It can be seen that the spectral efficiency of the proposed scheme degrades monotonically as the speed v_{max} is increased. Moreover, the performance improves with higher value of \bar{P} as observed also in Fig. 2. It can be noticed that the curves corresponding to IEEE 802.11ad do not show significant degradation as the speed is increased. This is due to the

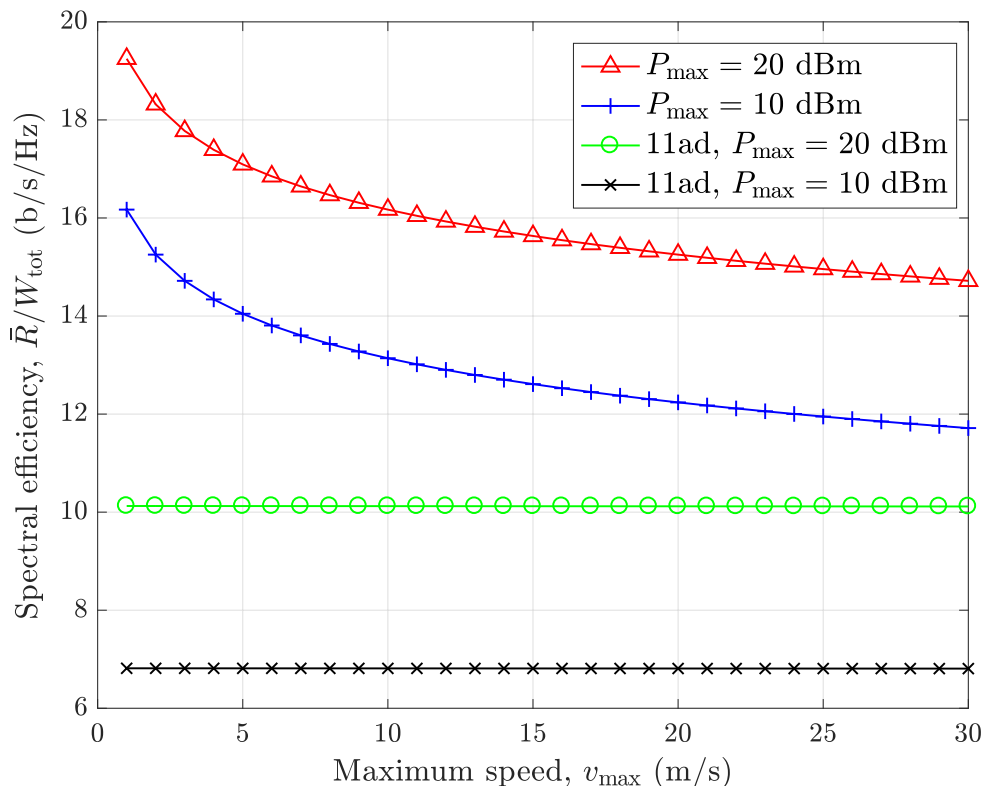


Fig. 3: Average spectral efficiency versus speed.

relatively wide beam used in IEEE 802.11ad, so that beam alignment is relatively infrequent. However, the performance of IEEE 802.11ad is poor compared to our proposed scheme.

V. CONCLUSION

In this paper, we propose a one-dimensional mobility model where a vehicle moves along a straight road with time-varying and random speed and communicates with base stations located on the roadside over the mm-wave band. We propose a beam-sweeping – data communication protocol and study its performance in closed form. We derive structural properties of the optimal design, based on which we design a bisection algorithm. We compare numerically our proposed design to an adaptation of IEEE 802.11ad to our model, which exhibits performance degradation up to 90%.

REFERENCES

- [1] J. Choi, V. Va, N. Gonzalez-Prelcic, R. Daniels, C. R. Bhat, and R. W. Heath, “Millimeter-wave vehicular communication to support massive automotive sensing,” *IEEE Communications Magazine*, vol. 54, no. 12, pp. 160–167, December 2016.

- [2] V. Va, T. Shimizu, G. Bansal, and R. W. Heath, “Beam design for beam switching based millimeter wave vehicle-to-infrastructure communications,” in *2016 IEEE International Conference on Communications (ICC)*, May 2016, pp. 1–6.
- [3] T. S. Rappaport, *Wireless communications: principles and practice*. Prentice Hall PTR, 2002.
- [4] M. R. Akdeniz, Y. Liu, M. K. Samimi, S. Sun, S. Rangan, T. S. Rappaport, and E. Erkip, “Millimeter Wave Channel Modeling and Cellular Capacity Evaluation,” *IEEE Journal on Selected Areas in Communications*, vol. 32, no. 6, pp. 1164–1179, June 2014.
- [5] C. Jeong, J. Park, and H. Yu, “Random access in millimeter-wave beamforming cellular networks: issues and approaches,” *IEEE Communications Magazine*, vol. 53, no. 1, pp. 180–185, January 2015.
- [6] V. Desai, L. Krzymien, P. Sartori, W. Xiao, A. Soong, and A. Alkhateeb, “Initial beamforming for mmWave communications,” in *48th Asilomar Conference on Signals, Systems and Computers*, Nov 2014, pp. 1926–1930.
- [7] M. Hussain and N. Michelusi, “Throughput optimal beam alignment in millimeter wave networks,” in *Information Theory and Applications Workshop (ITA)*, Feb 2017, pp. 1–6.
- [8] —, “Energy efficient beam alignment in millimeter wave networks,” in *2017 Asilomar Conference on Signals, Systems, and Computers*, 2017, to appear.
- [9] A. Alkhateeb, O. E. Ayach, G. Leus, and R. W. Heath, “Channel estimation and hybrid precoding for millimeter wave cellular systems,” *IEEE Journal of Selected Topics in Signal Processing*, vol. 8, no. 5, pp. 831–846, Oct 2014.
- [10] Z. Marzi, D. Ramasamy, and U. Madhow, “Compressive channel estimation and tracking for large arrays in mm-wave picocells,” *IEEE Journal of Selected Topics in Signal Processing*, vol. 10, no. 3, pp. 514–527, April 2016.
- [11] N. González-Prelcic, R. Méndez-Rial, and R. W. Heath, “Radar aided beam alignment in mmwave v2i communications supporting antenna diversity,” in *Information Theory and Applications Workshop (ITA)*, Jan 2016, pp. 1–7.
- [12] T. Nitsche, A. B. Flores, E. W. Knightly, and J. Widmer, “Steering with eyes closed: Mm-wave beam steering without in-band measurement,” in *2015 IEEE Conference on Computer Communications (INFOCOM)*, April 2015, pp. 2416–2424.
- [13] V. Va, J. Choi, T. Shimizu, G. Bansal, and R. W. Heath, “Inverse Multipath Fingerprinting for Millimeter Wave V2I Beam Alignment,” *IEEE Transactions on Vehicular Technology*, vol. PP, no. 99, pp. 1–1, 2017.
- [14] “IEEE Std 802.15.3c-2009,” *IEEE Standard*, pp. 1–200, Oct 2009.
- [15] “IEEE Std 802.11ad-2012,” *IEEE Standard*, pp. 1–628, Dec 2012.
- [16] V. Va, J. Choi, and R. W. Heath, “The Impact of Beamwidth on Temporal Channel Variation in Vehicular Channels and Its Implications,” *IEEE Transactions on Vehicular Technology*, vol. 66, no. 6, pp. 5014–5029, June 2017.
- [17] J. B. Kenney, “Dedicated short-range communications (dsrc) standards in the united states,” *Proceedings of the IEEE*, vol. 99, no. 7, pp. 1162–1182, July 2011.
- [18] M. Hussain, D. J. Love, and N. Michelusi, “Neyman-Pearson Codebook Design for Beam Alignment in Millimeter-Wave Networks,” in *Proceedings of the 1st ACM Workshop on Millimeter-Wave Networks and Sensing Systems*. New York, NY, USA: ACM, 2017, pp. 17–22.
- [19] S. Noh, M. D. Zoltowski, and D. J. Love, “Multi-Resolution Codebook and Adaptive Beamforming Sequence Design for Millimeter Wave Beam Alignment,” *IEEE Transactions on Wireless Communications*, vol. 16, no. 9, pp. 5689–5701, Sept 2017.
- [20] N. Michelusi and M. Hussain, “Optimal Beam Sweeping and Communication in Mobile Millimeter-wave Networks,” Purdue University, Tech. Rep., 2017, <https://engineering.purdue.edu/~michelus/ICC2018.pdf>.

APPENDIX A

PROOF OF THEOREM 1

Proof. First, note that if $\zeta = \hat{u}_{\text{comm}}(v, \eta)/v - 1$, then $\hat{P}(v(1 + \zeta), \eta, v) = 0 < P_{\text{max}}$ and $\hat{R}(v(1 + \zeta), \eta, v) = 0$. This configuration is clearly suboptimal since a non-zero rate can be achieved by increasing ζ .

Now, let $\hat{u}_{\text{comm}}(v, \eta)/v - 1 < \zeta < 0$ and assume this configuration is optimal. Note that this implies $v > \hat{u}_{\text{comm}}(v, \eta)$, or equivalently $v > \frac{1}{2} \frac{\eta^2 + 3\eta - 2}{\eta - 1}$.

We have two cases: 1) $v > \frac{1}{2}(\eta - 1)(\eta - 2)$ and 2) $v = \frac{1}{2}(\eta - 1)(\eta - 2)$ (and consequently $\eta \geq 5$ since we must also have $v > \frac{1}{2} \frac{\eta^2 + 3\eta - 2}{\eta - 1}$).

a) $v > \frac{1}{2}(\eta - 1)(\eta - 2)$: We show that, by increasing ζ and decreasing v so as to preserve the power consumption, the rate strictly increases, and thus we achieve a contradiction. From (22) and (23) with $\zeta < 0$ we obtain

$$\hat{R}(\eta, v, \zeta) = \frac{\eta}{\eta - 1} \frac{\hat{u}_{\text{comm}}(v, \eta)}{v + \frac{\eta}{2} - 1} \quad (40)$$

$$\times \left[\frac{v}{\hat{u}_{\text{comm}}(v, \eta)} (1 + \zeta) - 1 - \ln \left(\frac{v}{\hat{u}_{\text{comm}}(v, \eta)} (1 + \zeta) \right) \right],$$

$$\hat{P}(\eta, v, \zeta) = \frac{\eta \left(v(1 + \zeta) - \hat{u}_{\text{comm}}(v, \eta) \right)^2}{2(\eta - 1) \left(v + \frac{\eta}{2} - 1 \right)}. \quad (41)$$

We increase ζ by $h > 0$ (arbitrarily small) and decrease v by a function $g(h) > 0$, so as to maintain the power consumption unaltered, *i.e.*,

$$\hat{P}(\eta, v, \zeta) = \hat{P}(\eta, v - g(h), \zeta + h). \quad (42)$$

In the limit $h \rightarrow 0$ we must have

$$\frac{d\hat{P}(\eta, v, \zeta)}{d\zeta} - g'(0) \frac{d\hat{P}(\eta, v, \zeta)}{dv} = 0, \quad (43)$$

where $g'(0)$ is the derivative of $g(h)$ in zero, which must be positive since $g(h) > 0$ for arbitrarily small h . To show this, note that

$$\frac{d\hat{P}(\zeta, \eta, v)}{d\zeta} = \frac{\eta v \left(v(1 + \zeta) - \hat{u}_{\text{comm}}(v, \eta) \right)}{(\eta - 1) \left(v + \frac{\eta}{2} - 1 \right)} > 0, \quad (44)$$

$$\begin{aligned} \frac{d\hat{P}(\zeta, \eta, v)}{dv} &= \frac{\eta \left(v(1 + \zeta) - \hat{u}_{\text{comm}}(v, \eta) \right)}{2(\eta - 1) \left(v + \frac{\eta}{2} - 1 \right)^2} \\ &\times \left((1 + \zeta)(v + \eta - 2) - \frac{v}{\eta} + \frac{1}{2}\eta + \frac{1}{2} + \frac{1}{\eta} \right) > 0, \end{aligned} \quad (45)$$

where the last inequality follows from the fact that $\zeta > \hat{u}_{\text{comm}}(v, \eta)/v - 1$. Hence, it follows that indeed $g'(0) > 0$.

We now show that, for arbitrarily small h ,

$$\hat{R}(\eta, v, \zeta) < \hat{R}(\eta, v - g(h), \zeta + h). \quad (46)$$

Equivalently, in the limit $h \rightarrow 0$, we must have

$$\frac{d\hat{R}(\eta, v, \zeta)}{d\zeta} - g'(0) \frac{d\hat{R}(\eta, v, \zeta)}{dv} > 0. \quad (47)$$

Note that

$$\frac{d\hat{R}(\eta, v, \zeta)}{d\zeta} = \frac{1}{v(1 + \zeta)} \frac{d\hat{P}(\zeta, \eta, v)}{d\zeta}, \quad (48)$$

$$\begin{aligned} \frac{d\hat{R}(\zeta, \eta, v)}{dv} &= \frac{\eta(\eta/2 - 1)}{(\eta - 1)v \left(v + \frac{\eta}{2} - 1 \right)^2} [v(1 + \zeta) - \hat{u}_{\text{comm}}(v, \eta)] \\ &+ \frac{\eta(\eta/2 + 1)}{(\eta - 1) \left(v + \frac{\eta}{2} - 1 \right)^2} \ln \left(\frac{v}{\hat{u}_{\text{comm}}(v, \eta)} (1 + \zeta) \right), \end{aligned} \quad (49)$$

and thus replacing (48) in (47), and using (43) and the fact that $g'(0) > 0$, we obtain the equivalent condition

$$\frac{d\hat{P}(\eta, v, \zeta)}{dv} - v(1 + \zeta) \frac{d\hat{R}(\eta, v, \zeta)}{dv} > 0, \quad (50)$$

iff

$$g(\zeta) \triangleq \left(1 - \frac{\hat{u}_{\text{comm}}(v, \eta)}{v(1 + \zeta)}\right) \left((1 + \zeta)v - \frac{v}{\eta} + \frac{1}{2}\eta + \frac{1}{2} + \frac{1}{\eta}\right) - (\eta + 2) \ln \left(\frac{v}{\hat{u}_{\text{comm}}(v, \eta)}(1 + \zeta)\right) > 0, \quad (51)$$

which we are now going to prove. The derivative with respect to ζ is given by

$$\begin{aligned} \frac{dg(\zeta)}{d\zeta} &\propto \eta(v(1 + \zeta) - \hat{u}_{\text{comm}}(v, \eta))^2 \\ &+ (2v + \eta - 2)(v(1 + \zeta) - \hat{u}_{\text{comm}}(v, \eta)) > 0, \end{aligned} \quad (52)$$

where the inequality follows from the fact that $\zeta > \hat{u}_{\text{comm}}(v, \eta)/v - 1$. It follows that $g(\zeta)$ is an increasing function of ζ , minimized at $\zeta = \hat{u}_{\text{comm}}(v, \eta)/v - 1$, thus proving the inequality.

b) $v = \frac{1}{2}(\eta - 1)(\eta - 2)$ and $\eta \geq 5$: In this case, we cannot decrease v any further. Using a similar approach as in the previous case, we show that a strictly larger rate can be obtained by decreasing both η and ζ , while preserving the power consumption. From (40) and (41) with $v = \frac{1}{2}(\eta - 1)(\eta - 2)$, we obtain

$$\hat{R}(\eta, v, \zeta) = 1 + \zeta \quad (53)$$

$$- \frac{2\eta}{(\eta - 1)(\eta - 2)} \left[1 + \ln \left(\frac{(\eta - 1)(\eta - 2)(1 + \zeta)}{2\eta} \right) \right],$$

$$\hat{P}(\eta, v, \zeta) = \frac{[v(1 + \zeta) - \hat{u}_{\text{comm}}(v, \eta)]^2}{(\eta - 1)(\eta - 2)}, \quad (54)$$

where $\frac{-\eta^2 + 5\eta - 2}{(\eta - 1)(\eta - 2)} < \zeta < 0$.

Now, we decrease η by one unit, while keeping v as before, and we choose the new ζ , denoted as $\hat{\zeta}$, in such a way as to preserve the power consumption. Note that $v \geq v_{\min}(\eta - 1)$ hence the constraint on v is still satisfied, since $v_{\min}(\eta - 1)$ is a decreasing function of η .

From (41) with $v = \frac{1}{2}(\eta - 1)(\eta - 2)$ we obtain

$$\hat{P}(\eta - 1, v, \hat{\zeta}) = \frac{(\eta - 1) \left(v(1 + \hat{\zeta}) - \hat{u}_{\text{comm}}(v, \eta - 1) \right)^2}{(\eta - 2)(\eta^2 - 2\eta - 1)}. \quad (55)$$

where

$$\hat{u}_{\text{comm}}(v, \eta - 1) = \eta - \frac{1}{\eta - 1} < \hat{u}_{\text{comm}}(v, \eta) = \eta. \quad (56)$$

$\hat{\zeta}$ is chosen so that $\hat{P}(\eta - 1, v, \hat{\zeta}) = \hat{P}(\eta, v, \zeta)$, yielding

$$\begin{aligned} v(1 + \hat{\zeta}) &= \hat{u}_{\text{comm}}(v, \eta - 1) \\ &+ \sqrt{\eta^2 - 2\eta - 1} \frac{v(1 + \zeta) - \hat{u}_{\text{comm}}(v, \eta)}{\eta - 1}. \end{aligned} \quad (57)$$

Thus, it follows that $v(1 + \hat{\zeta}) > \hat{u}_{\text{comm}}(v, \eta - 1)$. Additionally, using (56) and the fact that $v(1 + \zeta) - \hat{u}_{\text{comm}}(v, \eta) > 0$ it follows that $v(1 + \hat{\zeta}) < v(1 + \zeta)$. Therefore

$$\hat{u}_{\text{comm}}(v, \eta - 1) < v(1 + \hat{\zeta}) < v(1 + \zeta) < v, \quad (58)$$

since $\zeta < 0$, hence $\hat{u}_{\text{comm}}(v, \eta - 1)/v - 1 < \hat{\zeta} < 0$. We now show that this new configuration strictly increases the throughput. From (40) and using the expression of $\hat{\zeta}$ and of $\hat{u}_{\text{comm}}(v, \eta - 1)$ we obtain

$$\begin{aligned} \hat{R}(\eta - 1, v, \hat{\zeta}) &= \frac{2}{(\eta - 2)\sqrt{\eta^2 - 2\eta - 1}}(v(1 + \zeta) - \eta) \\ &- \frac{2(\eta^2 - \eta - 1)}{(\eta - 2)(\eta^2 - 2\eta - 1)} \ln(v(\hat{\zeta} + 1)/\hat{u}_{\text{comm}}(v, \eta - 1)), \end{aligned} \quad (59)$$

and therefore

$$\begin{aligned} h(\zeta) &\triangleq \hat{R}(\eta - 1, v, \hat{\zeta}) - \hat{R}(\eta, v, \zeta) \\ &= \frac{4(v(1 + \zeta) - \eta)}{(\eta - 1)(\eta - 2)\sqrt{\eta^2 - 2\eta - 1}(\eta - 1 + \sqrt{\eta^2 - 2\eta - 1})} \\ &+ \frac{2\eta}{(\eta - 1)(\eta - 2)} \ln(v(1 + \zeta)/\eta) \\ &- \frac{2(\eta^2 - \eta - 1)}{(\eta - 2)(\eta^2 - 2\eta - 1)} \ln(v(\hat{\zeta} + 1)/\hat{u}_{\text{comm}}(v, \eta - 1)). \end{aligned} \quad (60)$$

The derivative of $h(\zeta)$ with respect to ζ is given by

$$\begin{aligned} \frac{dh(\zeta)}{d\zeta} &\propto v(1 + \zeta) - \hat{u}_{\text{comm}}(v, \eta) \\ &+ \frac{2(v(1 + \zeta) - \eta)^2}{\eta - 1 + \sqrt{\eta^2 - 2\eta - 1}} > 0. \end{aligned} \quad (61)$$

Therefore, $h(\zeta)$ is an increasing function of ζ , minimized at $\zeta = \hat{u}_{\text{comm}}(v, \eta)/v - 1$, yielding

$$\hat{R}(\hat{\zeta}, \eta - 1, v) - \hat{R}(\zeta, \eta, v) > 0. \quad (62)$$

The Theorem is thus proved. □

APPENDIX B

PROOF OF THEOREM 2

Proof. To study the optimization problem **P3**, we study the derivative $\hat{R}(\eta, v, \zeta(v, \eta))$ with respect to v . We have that

$$\begin{aligned} \frac{d\hat{R}(\eta, v, \zeta(v, \eta))}{dv} &= \frac{d\hat{R}(\eta, v, \zeta)}{dv} + \frac{d\hat{R}(\eta, v, \zeta)}{d\zeta} \frac{d\zeta(v, \eta)}{dv} \\ &\propto f_\eta(v), \end{aligned} \tag{63}$$

where \propto denotes proportionality up to a positive multiplicative factor, with $f_\eta(v)$ given by (36). Therefore, $\hat{R}(\zeta, \eta, v)$ is an increasing function of v iff $f_\eta(v) > 0$. We now show that $f_\eta(v)$ is a strictly decreasing function of v , with limits given by (37).

Note that \hat{v} can be determined using the bisection method. In fact, $f_\eta(v)$ is a decreasing function of v (see proof of the theorem), with

$$\lim_{v \rightarrow \frac{1}{2} \frac{\eta^2 + 3\eta - 2}{\eta - 1}} f_\eta(v) = \infty \tag{64}$$

and

$$f_\eta(v_{\max}(\eta)) < 0 \tag{65}$$

(see second part of the proof). Therefore, there exists a unique $\hat{v} \in (\frac{1}{2} \frac{\eta^2 + 3\eta - 2}{\eta - 1}, v_{\max}(\eta))$ such that $f_\eta(\hat{v}) = 0$, and $\frac{d\hat{R}(\eta, v, \zeta(v, \eta))}{dv} > 0$ for $v < \hat{v}$ and $\frac{d\hat{R}(\eta, v, \zeta(v, \eta))}{dv} < 0$ for $v > \hat{v}$.

Therefore, the maximum of $\hat{R}(\eta, v, \zeta(v, \eta))$ with respect to $v \in (\frac{1}{2} \frac{\eta^2 + 3\eta - 2}{\eta - 1}, v_{\max}(\eta))$ is attained at $v = \hat{v}$. By combining this result with the constraint $v \geq v_{\min}(\eta)$, we obtain (35).

Thus, we now show that $f_\eta(v)$ is a decreasing function of v . We have

$$\begin{aligned}
& (1 + \zeta(v, \eta))^2 \frac{df_\eta(v)}{dv} \\
&= -(\eta - 1) \frac{(\eta - 1)(v + \eta/2 - 1) + 2\eta}{2v\eta^2} (1 + \zeta(v, \eta)) \\
&+ [v - \hat{u}_{\text{comm}}(v, \eta)] \frac{(\eta - 1)(\eta/2 - 1) + 2\eta}{2v^2\eta} (1 + \zeta(v, \eta)) \\
&+ [v - \hat{u}_{\text{comm}}(v, \eta)] \frac{(\eta - 1)(v + \eta/2 - 1) + 2\eta}{2v\eta} \zeta'(v, \eta) \\
&- \frac{(\eta - 1)}{\eta} \zeta(v, \eta) (1 + \zeta(v, \eta)) - \frac{(\eta - 1)(v + \eta/2 - 1)}{\eta} \zeta'(v, \eta) \\
&+ \eta \zeta'(v, \eta) (1 + \zeta(v, \eta)) \\
&+ [1/v - 1/\hat{u}_{\text{comm}}(v, \eta)/\eta] (\eta/2 + 1) (1 + \zeta(v, \eta))^2, \tag{66}
\end{aligned}$$

where $\zeta'(v, \eta) = \frac{d\zeta(v, \eta)}{dv}$. By simplifying and reorganizing the expression, we obtain

$$\begin{aligned}
& (1 + \zeta(v, \eta))^2 \frac{df(v)}{dv} = -\frac{1}{v} [v - \hat{u}_{\text{comm}}(v, \eta)]^2 \\
&\times \left[\frac{\eta + 2}{2\eta v \hat{u}_{\text{comm}}(v, \eta)} + \frac{v - \hat{u}_{\text{comm}}(v, \eta)}{4v(v + \eta/2 - 1)} \right] \tag{67} \\
&- \zeta(v, \eta) \frac{[v - \hat{u}_{\text{comm}}(v, \eta)]}{v^2} \\
&\times \left[\frac{\eta^2/2 + 3/2\eta - 1}{v - \hat{u}_{\text{comm}}(v, \eta)} + \frac{\eta^3}{(v + \eta/2 - 1)(\eta - 1)} + \frac{(\eta + 2)v}{\eta \hat{u}_{\text{comm}}(v, \eta)} \right] \\
&- \zeta(v, \eta) \frac{[v - \hat{u}_{\text{comm}}(v, \eta)]^2}{v^2} \left[1 + \frac{\eta^2 + 3\eta - 2}{2(v + \eta/2 - 1)(\eta - 1)} \right] \\
&- \zeta(v, \eta)^2 \frac{1}{v} \left[[v/\hat{u}_{\text{comm}}(v, \eta) - 1](1/2 + 1/\eta) \right. \\
&+ \left. \frac{\eta^2}{(v + \eta/2 - 1)(\eta - 1)} \frac{\eta^2/2 + 3/2\eta - 1}{v - \hat{u}_{\text{comm}}(v, \eta)} \right] \\
&- \zeta(v, \eta)^2 \frac{1}{v} \left[\frac{v - \hat{u}_{\text{comm}}(v, \eta) + 2\eta}{(v + \eta/2 - 1)(\eta - 1)} \eta^2 + 1 + v - \hat{u}_{\text{comm}}(v, \eta) \right] < 0, \tag{68}
\end{aligned}$$

where inequality holds since $\zeta(v, \eta) \geq 0$ and $v > \hat{u}_{\text{comm}}(v, \eta)$. This proves that $f_\eta(v)$ is strictly decreasing in v .

Now, note that, in the limit $v \rightarrow \frac{1}{2} \frac{\eta^2 + 3\eta - 2}{\eta - 1}$, we obtain $v \rightarrow \hat{u}_{\text{comm}}(v, \eta)$ and $\zeta(v, \eta) \rightarrow \infty$, yielding (64). On the other hand, when $v = v_{\text{max}}(\eta)$, by letting $x \triangleq \hat{P}_{\text{max}}(\eta - 1)[1 +$

$\sqrt{1 + 2\eta/\hat{P}_{\max}} > 0$ we obtain

$$f_{\eta}(v_{\max}(\eta)) = -(\eta - 1) \frac{x[\eta + 2 + x]}{\eta^2 + 3\eta - 2 + 2\eta x} \quad (69)$$

$$+ \ln \left(1 + \frac{(\eta - 1)x}{\eta^2/2 + 3/2\eta - 1 + x} \right) (\eta/2 + 1) \triangleq g(x). \quad (70)$$

The derivative of the above expression with respect to x satisfies

$$\frac{dg(x)}{dx} \propto -[\eta^2/2 + 3/2\eta - 1][2\eta + 2x + x\eta] - x^2\eta < 0, \quad (71)$$

which satisfies the inequality since $\eta \geq 2$, hence $g(x)$ is maximized at $x = 0$, yielding

$$f_{\eta}(v_{\max}(\eta)) = g(x) < g(0) = 0. \quad (72)$$

The Theorem is thus proved. □